Available online at www.sciencedirect.com
ScienceDirect
C. R. Physique 9 (2008) 585–594
COMPTES RENDUS PHYSIQUE
http://france.elsevier.com/direct/COMREN/

Synchrotron x-rays and condensed matter/Rayonnement X synchrotron et matière condensée

Magnetization dynamics: ultra-fast and ultra-small

Yves Acremann

PULSE Center, Stanford Linear Accelerator Center, 2575 Sand Hill Road, Menlo Park, CA 94025, USA

Available online 23 October 2007

Abstract

Ultrafast magnetic processes are of great scientific interest but also form the basis of high density magnetic recording applications. We demonstrate the uniqueness of time resolved, high resolution magnetic X-ray microscopy, and show that the motion of a magnetic vortex core can be imaged. The vortex core direction is hidden to most experimental techniques, but has a decisive influence on the dynamics of the magnetic structure.

We imaged the switching of a ferromagnetic nanostructure by a spin polarized current pulse using time resolved X-ray microscopy. As opposed to the common uniform switching process due to Néel and Stoner–Wohlfarth, the magnetization in spin injection devices does not switch uniformly, but involves the motion of a magnetic vortex. ***To cite this article: Y. Acremann, C. R. Physique 9 (2008).***

© 2007 Académie des sciences. Published by Elsevier Masson SAS. All rights reserved.

Résumé

Dynamique de magnétisation : ultra-rapide et ultra-petit. Les processus magnétiques ultra-rapides sont d'un grand intérêt scientifique mais ils sont aussi à la base des applications en matière d'enregistrement magnétique à haute densité. Nous démontrons les capacités uniques de la microscopie X magnétique à haute résolution et résolue en temps et prouvons que le mouvement du cœur d'un vortex magnétique peut être imagé. La direction prise par le cœur reste inaccessible à la plupart des techniques expérimentales mais elle a une influence déterminante sur la dynamique de la structure magnétique.

A l'aide de la microscopie X résolue en temps, nous avons imagé le basculement d'une nanostructure ferromagnétique induit par une impulsion de courant polarisée en spin. A la différence du processus habituel de basculement décrit par Néel et Stoner–Wohlfarth, la magnétisation des dispositifs à injection de spin ne bascule pas uniformément mais implique le déplacement d'un vortex magnétique. ***Pour citer cet article : Y. Acremann, C. R. Physique 9 (2008).***

© 2007 Académie des sciences. Published by Elsevier Masson SAS. All rights reserved.

Keywords: Magnetism; Ultrafast Microscopy; Synchrotron radiation

Mots-clés : Magnétisme ; Microscopie ultra-rapide ; Rayonnement synchrotron

1. Magnetism and its time and length scales

Many physical concepts have been learned from magnetism, for example the concept of a field or of phase transitions. More recent experiments explore magnetism far from thermal equilibrium by looking at the response of the magnetization to a field or heat pulse. Surprisingly, magneto-dynamics stretches over many orders of magnitude in

E-mail address: acremann@slac.stanford.edu.

1631-0705/$ – see front matter © 2007 Académie des sciences. Published by Elsevier Masson SAS. All rights reserved.
doi:10.1016/j.crhy.2007.05.017

time and space. The typical time scale of magnetization precession in a magnetic field of 1 Tesla is on the order of picoseconds, whereas the data retention time on a computer hard disk is designed to be at least 10 years. Associated with sub-nanosecond time scales are short length scales as the propagation speed of spin waves is of the order of the speed of sound.

Currently, magnetism research is strongly driven by the technological need of faster and smaller nonvolatile memory devices. The length scales used in storage applications have reached the nanoscale. Typical bits on a hard disk have a size of <100 nm. Each bit consists of hard magnetic grains. These grains are typically 10 nm in size and recent developments will lead to even smaller grains and bits. A novel technology uses magnetic particles to store information in a solid state memory device which is envisioned to bridge the gap in speed and access time between random access memory and a hard disk. The size of a bit on such a magnetic random access memory (MRAM) device is on the order of 100 nm as well. As technology reaches deep into the nanometer length scale, bits are written on the nanosecond time scale, using dynamic processes on a time scale of a few 100 ps.

X-ray microscopy using synchrotron radiation [1–3] uniquely combines the length scale of sub 100 nm with the time scale of 100 ps. No other technique in magnetism offers this possibility. Many microscopy techniques offer an extremely high spatial resolution, such as spin polarized SEM [4,5], spin-STM [6,7] or magnetic force microscopy [8]. However, these techniques lack time resolution beyond the time scale of seconds. On the other hand, optical methods offer femtosecond time resolution. Time resolved scanning Kerr microscopy [9–13] and time resolved Kerr imaging [14] unveiled the microscopic nature of magnetization precession as well as magnetization reversal [15–18] in confined ferromagnetic structures. However, the spatial resolution is limited to the wavelength of visible light. Magnetic scanning near field optical microscopy is still under development [19].

2. The magnetic vortex: a hidden parameter in magnetism

Soft magnetic thin films (thinner than the magnetic exchange length) with low surface and crystalline anisotropy generally form planar magnetic domains. A typical domain structure of a thin rectangular magnetic element is the Landau pattern. The magnetization M forms four domains which are arranged with a sense of rotation around the center of the structure, collectively compensating the stray field of each individual domain. The reduction of the stray field energy needs to be compared to the exchange energy stored in the domain walls. Close to the crossing point of the domain walls, the exchange energy density grows dramatically. The total energy can be reduced further by the formation of a magnetic vortex in the center. In a magnetic vortex, the magnetization has an out of plane component near its center. In the center, M is perpendicular to the plane. There are two possibilities for the magnetization direction of this vortex core: it can point out or into the plane of the sample. The observation of the magnetic vortex core is very difficult as its small size requires high spatial resolution. A vortex core has been imaged by AFM [20] and spin polarized STM experiments [21], showing a vortex core size of $\approx$10 nm in Fe. Therefore, the direction of a vortex core remains a 'hidden parameter' for most experimental techniques. In the following experiments, we will see that the vortex, although small, can have a significant influence on the dynamics beyond the size of the vortex core.

2.1. Imaging of vortex driven magnetization dynamics

In this experiment [22], the motion of a magnetic vortex caused by a pulsed magnetic field was observed using time resolved photo emission electron microscopy (PEEM) [1]. The magnetic structures are patterned on a coplanar waveguide structure on a GaAs substrate. The waveguide is used to apply magnetic field pulses to the magnetic patterns in the plane of the film. The field pulse is generated by a current pulse from a photo conductive switch which is integrated into the sample by optical lithography and lift-off processing. The CoFe layer used as the ferromagnet has a thickness of 20 nm and has been patterned into rectangles of 1.5 μm × 1 μm.

A Ti-Sapphire laser has been synchronized to the 500 MHz radio frequency of the synchrotron source (Fig. 1). The pulsed laser beam triggered the photo conductive switch on the sample. During the experiment, the synchrotron was running in a special mode where only two electron buckets are filled, leading to a low pulse repetition rate. The repetition rate of the laser of 125 MHz leads to current pulses every 8 ns exciting the sample. Every time point within the 8 ns between two excitation pulses can be probed separately. To detect the magnetization, the circularly polarized X-ray beam of a bending magnet illuminates the magnetic structure on the sample. The magnetic contrast is provided by the magnetic circular dichroism effect (XMCD) at the L edges of the ferromagnetic material. Details

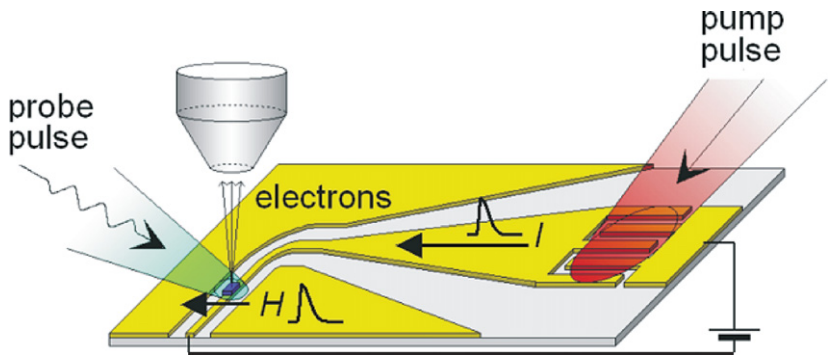

Fig. 1. Experimental setup to observe magneto dynamics using the photo electron emission microscope (PEEM). The magnetic sample is located on a waveguide structure used to apply a magnetic field pulse. The current pulse leading to the field pulse is generated by a photoconductive switch which is driven by a Ti:Sapphire laser oscillator. The laser is synchronized to the pulse repetition rate of the synchrotron source by a phase locked loop. The X-ray pulses of the synchrotron reach the sample at a well defined time τ after the current pulse and excite photo electrons. The photo electrons are imaged onto a CCD detector by electron optics.

of the experiment can be found in the original paper [22]. Each magnetic image contains the average of millions of pump-probe cycles. Therefore, we only see the repeatable part of the magnetization response to the pulse.

Fig. 2A shows the domain structures of two magnetic patterns. Both have the same in plane Landau domain structures. Fig. 2B shows the derivative of the magnetic contrast in order to improve the visibility of the domain walls. At the crossing point of the domain walls, we expect the formation of a magnetic vortex. However, the vortex core is not visible due to the limited spatial resolution of the PEEM microscope of $\approx$100 nm. Cross correlation of the gradient images was used to trace the position of the vortex as a function of time. Notice that the position of the vortex can be traced with a precision beyond the intrinsic resolution of PEEM because of the strong magnetic contrast and low image noise. Figs. 2C, D show the motion of the vortex as a function of time. We observe two phases of vortex dynamics: an initial linear acceleration in response to the field pulse, followed by a gyroscopic rotation driven by the in-plane magnetostatic field of the excited vortex. The vortex in Fig. 2C initially moves almost parallel to the applied magnetic field, whereas the vortex in Fig. 2D moves in the opposite direction. In addition, the gyroscopic rotation is opposite for the two vortices. This is surprising as the in-plane domain structure of the two structures is the same. Therefore, there must be a 'hidden parameter' present that rules the sub-nanosecond dynamical response of the vortex. The hidden parameter is the direction of the out of plane magnetization of the vortex core which is invisible to this and most other magnetic microscopy techniques. The gyroscopic motion is slow compared to typical precession frequencies of several GHz. Therefore, the sample has not fully relaxed before the next field pulse was applied. The magnitude of the gyroscopic motion is amplified further by resonant excitation as the sample does not fully relax between two field pulses.

Fig. 3 illustrates the spin structure of the left handed and right handed vortices. Intuitively, one expects an external magnetic field H to result in the growth of domain 4, which is aligned with the field. This would lead to an initial vortex displacement perpendicular to H. Experimentally, however, we observe an initial motion along the field pulse. The vortex center moves parallel or anti-parallel to the field because, on the sub-nanosecond time scale, magnetic moment precession around the field direction dominates over damping in the field direction. When viewed along the direction of the external field H, the magnetic moments experience a clockwise precessional torque along the H direction. In a left-handed vortex, the magnetization in domain 3 precesses in the direction of the core magnetization, which itself precesses in the direction of the magnetization in domain 1. This corresponds to a motion of the vortex core anti-parallel to the applied field. In contrast, for a right-handed vortex, the magnetization in domain 1 precesses in the direction of the core magnetization, resulting in a parallel motion. The vortex center thus controls the fast, precessional dynamics of a micron-scale vortex pattern. The displacement of the core after the field pulse powers the gyrotropic motion of the vortex [23]. The imbalance of the in-plane magnetization creates a magnetostatic field perpendicular to the displacement, which drives the vortex on a spiraling trajectory.

The domain walls of the Landau structure can lead to additional forces on the vortex as they move perpendicular to an applied field pulse. Especially in larger structures, the magnetization far away from the vortex as well as the dynamics of the domain walls can dominate over the dynamics of the vortex core. This may explain the experimental

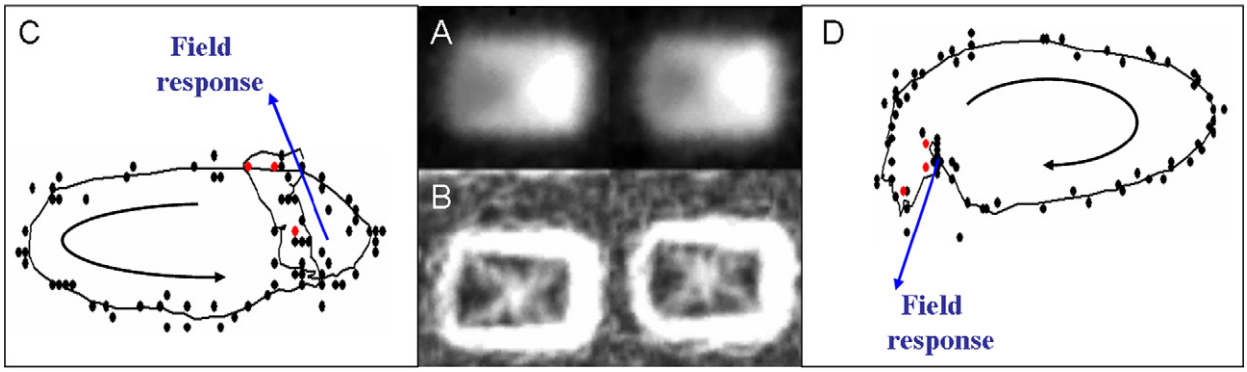

Fig. 2. (A) shows the static domain configuration of two ferromagnetic rectangles of 1.5 μm × 1 μm size. Both samples show an identical Landau flux closure structure. In (B), the domain walls have been made visible by calculating the derivative of M. (C) and (D) show the trajectory of the vortex center. Surprisingly, the vortex centers of the two structures move in opposite direction although they show the same Landau domain structure.

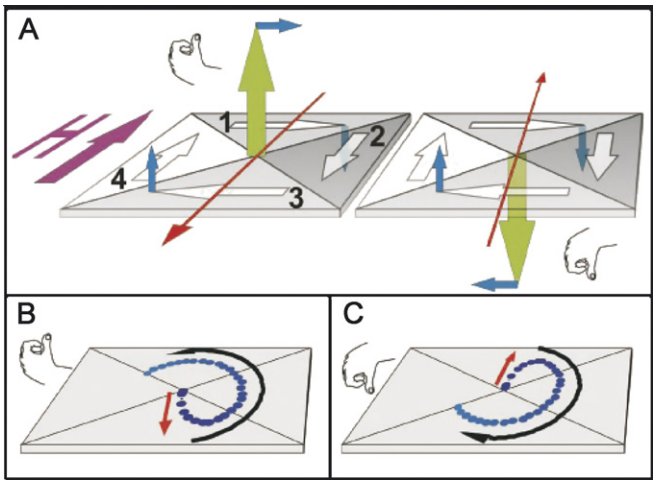

Fig. 3. (A) Spin structure of a left and right handed vortex structure. The blue arrows represent the precessional motion of the magnetization caused by the magnetic field pulse. The magnetization direction of the vortex center determines the initial direction of vortex motion parallel or anti-parallel to the magnetic field pulse. (B) and (C) show the simulated trajectory for two magnetization directions of the vortex core.

results found by Raabe et al. [24] where the dynamic response of a much larger magnetic structure was observed. In addition, a high spatial resolution is needed to detect the small circular motion of the vortex core [25].

2.2. *Resonant switching of a magnetic vortex core*

A magnetic vortex is very stable with respect to static magnetic fields and has a concentrated magnetic stray field originating from the core. Therefore, it is envisaged as a potential structure to store information. However, the required static switching field of the order of 0.5 T [26] is too large for practical applications. Yet, in a recent experiment by van Waeyenberge et al. [27], switching of a vortex core by an alternating AC magnetic field of only 1.5 mT has been demonstrated and will be described here.

The sample consists of a Permalloy element of 1.5 μm × 1.5 μm × 50 nm size patterned onto a waveguide structure. An AC current of 250 MHz was applied to the waveguide, leading to an oscillating magnetic field of 0.1 mT in the plane of the sample. The phase of the AC magnetic field has been locked to the 500 MHz bunch frequency of the synchrotron. The temporal evolution of the gyroscopic motion of the vortex at the crossing point of the domain walls was imaged by scanning transmission X-ray microscopy (STXM). A more detailed description of the experimental technique can be found in the original paper [27].

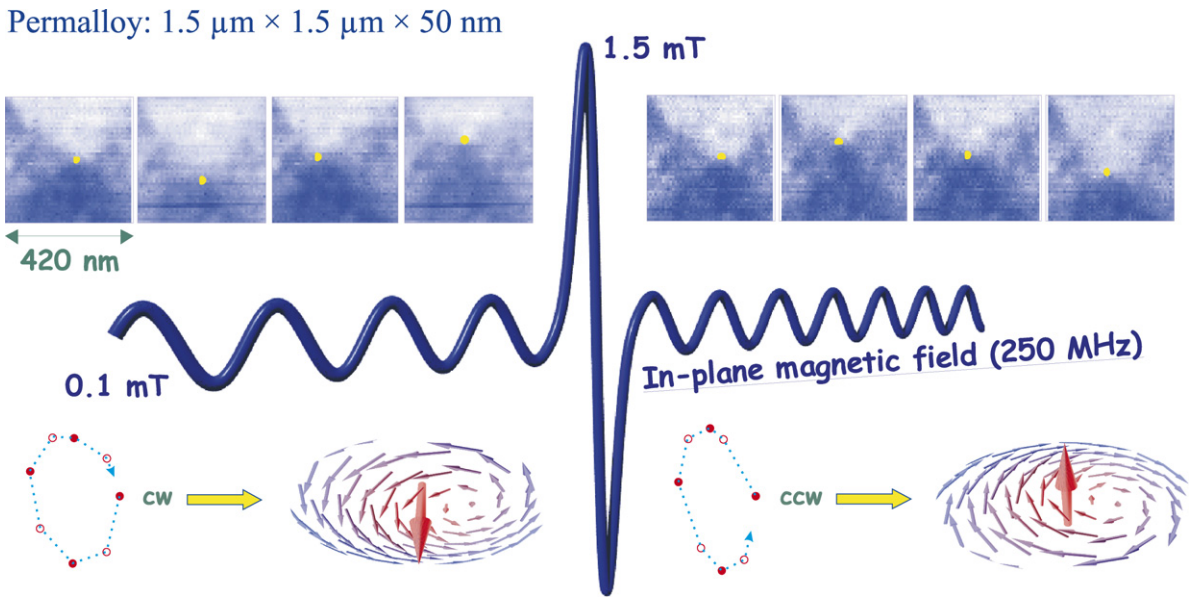

Fig. 4. Images of the vortex motion in an AC magnetic field with the vortex pointing into the sample plane (left) and out of the sample plane (right). A mono cycle of 1.5 mT AC magnetic field is enough to switch the magnetization of the vortex core, leading to the reversal of the vortex motion. (Courtesy of H. Stoll et al. [27].)

As the 0.1 mT sinusoidal magnetic field was applied, the gyroscopic motion of the vortex was observed as expected. However, when a short magnetic field burst of 4 ns and only 1.5 mT amplitude was applied, the sense of gyroscopic motion reversed (Fig. 4). Subsequent application of the RF burst leads to reversal of the sense of motion. As the sense of motion is directly linked to the magnetization of the vortex core, one can conclude that the magnetization direction of the vortex core was reversed. This offers a way to reverse the magnetization of a vortex on a sub-nanosecond time scale using a magnetic field that is 300 times weaker than the field required for switching by a static field.

3. Imaging spin transfer switching by X-ray microscopy

Magnetization reversal by injection of a spin current has been proposed by Slonczewski [28] and Berger [29]. Magnetization dynamics by spin injection has been demonstrated by various groups [30–44]. All spin transfer experiments so far used magneto-resistance effects to probe the magnetic state of the samples. The most common structures used to observe spin transfer effects are current perpendicular to plane (CPP) spin valves. Two ferromagnetic layers are separated by a thin Cu layer in a pillar like structure. The ends of the pillar are attached to thick contacts used to supply a charge current through the pillar as well as disperse heat generated by the current. One of the two ferromagnets is thin and intended to be switched (the 'free' layer) whereas the thicker ferromagnet is intended not to change its magnetization and to act as a spin current source ('fixed' layer).

A spin polarized current is generated by passing a current through the fixed layer. In a ferromagnet, the conductivity for electrons with their spins parallel to the magnetization differs from the conductivity for the opposite spin direction. Passing a current across an interface between a ferromagnet and a copper contact leads to a spin polarized current and the build-up of a spin voltage. This spin current passes through the free layer where precession [45] leads to a torque on the magnetization [28]. Similarly, a torque acts on the free layer if a current moves electrons from the free to the fixed layer.

Spin injection is one of the most interesting developments of magnetism as the direct import of angular momentum into a ferromagnet leads to new and unexpected effects. In certain geometries, spin injection effects cause a torque on the magnetization which acts like negative damping or the amplification of spin waves.

The main difficulty performing experiments on spin transfer switching lies in two aspects. First, the spin polarized charge current I_c creates a strong Oersted magnetic field $H_{\mathrm{Oe}} = \mu_0 \frac{I_c}{2\pi r}$ around the pillar of radius r. The spin torque T_s on a ferromagnet is proportional to the spin current density $j_s \propto T_s \propto \frac{I_c}{\pi r^2}$. For pillars with a diameter of ≈100 nm

or smaller, the spin torque dominates the torque caused by the Oersted field. Second, the current density needed for switching is around 10^7–10^8 A/cm^2. In a macroscopic sample, ohmic heating would lead to sample destruction whereas scaling to nanostructures makes these experiments possible due to a more favourable surfact to volume ratio.

So far, all experimental knowledge on spin transfer switching comes from transport experiments which provide information about the relative average magnetization difference between the free and fixed layer. The small scale of spin transfer devices as well as the fact that the free layer is buried under thick contacts rules out all conventional magnetic microscopy techniques to observe the inner magnetization structure of the free layer. So far, only scanning transmission X-ray microscopy (STXM) [2] is adequate to observe the dynamics of the switching process in space and time for the following reasons:

- Typical metal films of several tens of nanometers used in spin transfer devices are transparent for soft X-rays. This allows one to image deeply buried magnetic layers.
- The X-ray beam of the synchrotron source is pulsed with a pulse length of <100 ps, providing the time resolution needed to observe the switching process.
- The topographic contrast of the pillar is located close to the magnetic contrast. Therefore, lock-in detection schemes are required to measure the magnetic contrast independently of sample topography. The STXM uses a point detector which can be read out fast and is suited for lock-in detection.

Our sample consisted of a 4 nm thick free layer with an elliptical cross section of 100 nm $\times$ 150 nm, sandwiched between other layers and buried under current leads in a typical current perpendicular to plane spin valve pillar, as illustrated in Fig. 5. Current pulses of 2×10^8 A/cm^2 provided by a pulse generator flow perpendicular to the pillar from the top to the bottom or vice versa, depending on the sign of the voltage applied to the Cu electrodes. The free layer consists of $Co_{0.86}Fe_{0.14}$. The multilayer structure below the free layer is designed to spin polarize the current while minimizing magnetic coupling to the free layer.

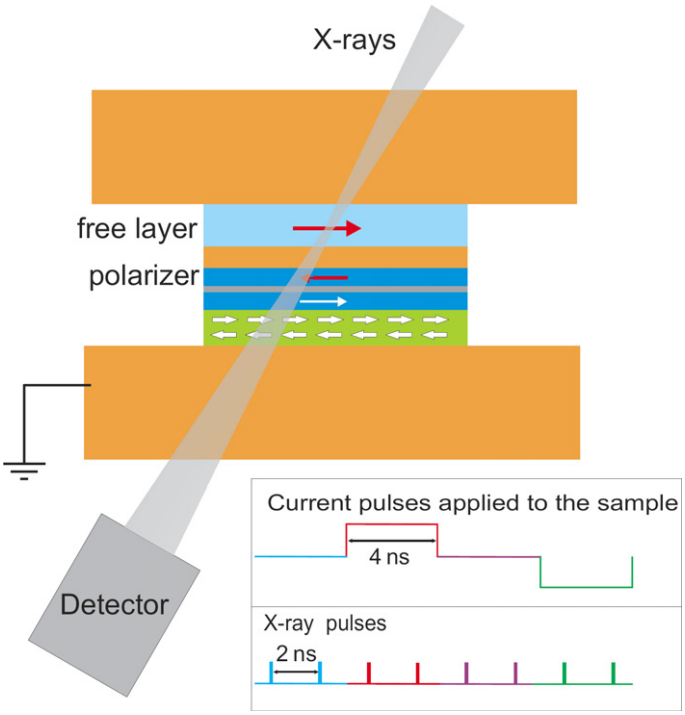

Fig. 5. The experimental setup to image the switching process in a spin transfer pillar device. The pillar structure is shown including the Cu contacts on top and bottom. The incident monochromatic X-ray beam is focused and the transmitted intensity is measured as a function of the beam position. The pump-probe timing scheme is shown at the bottom.

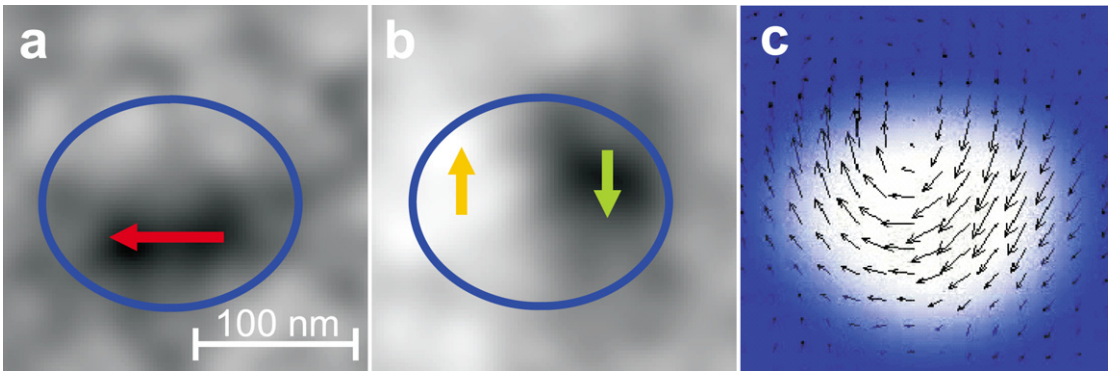

Fig. 6. Magnetic images and the reconstruction of the magnetization vectors. (a) shows the magnetic contrast along the x direction where (b) shows the contrast along y. The arrows in (c) are constructed from (a) and (b).

Images of $M(x, y, t)$, where x and y are coordinates in the plane of the free layer and t is the time, are obtained by scanning the sample through the focus of the zone plate, as shown in Fig. 5. The circularly polarized X-ray beam from the undulator on beam line 11.0.2 at the Advanced Light Source (ALS) is incident 30° from the surface normal. It is focused to ≈30 nm by a zone plate. The transmission of the X-rays through the whole pillar is monitored by a fast avalanche detector as a function of the position (x, y) while the pillar is scanned in steps of 10 nm across the X-ray focus. Tuning the photon energy to the characteristic Co L_3 resonance provides magnetic contrast through the X-ray magnetic circular dichroism (XMCD) effect.

M_x and M_y components of M are obtained by rotating the pillar by 90° in the x–y plane. 4 ns positive (set) and 4 ns negative (reset) current pulses separated by 4 ns are applied to the sample by two pulse generators. The rise time of the current pulses is 200 ps. The current pulse sequence is synchronized with the X-ray pulses, which appear every 2 ns. A special photon counting system [46] allows us to measure the differences of the magnetizations $M_i - M_j$ for each pair of eight consecutive X-ray pulses. This allows us to reliably suppress the topographic background from the pillar. The delay of the 75 ps wide X-ray pulses to the current pulse sequence can be adjusted in order to measure the time evolution of the magnetization. The magnetization of the free layer can be reconstructed from transport experiments which show that the initial magnetization state of the free layer is uniform. The uniform state is also reached at the end of the pulse sequence.

As an example, Fig. 6 shows the spatial variation of $M = (M_x, M_y)$, recorded 2 ns after the rising edge of the set-current pulse. The length of the arrows represents the XMCD contrast from the combined orthogonal images in the x (horizontal) and y (vertical) directions. Note that the length of the arrows is influenced by the spatial resolution. To our knowledge, this is the first time that the magnetic structure in a spin injection pillar has been observed. Obviously, the magnetization is not uniform but is bent into a C state, influencing the dynamics of the switching process.

The time evolution of the magnetization near the onset of the current pulses reveals a novel magnetization switching mechanism and is shown in Figs. 7(a)–(i). The initial magnetization is uniform (Fig. 7(a)). The positive current pulse causes the magnetization to bend upwardly (Fig. 7(b)), forming a vortex. As this vortex moves through the free layer, it leaves behind a trail of reversed magnetization. As the vortex center leaves the magnetic structure, a C state (Fig. 7(c)) is formed. The end of the positive set pulse has no noticeable effect, showing that the C state (Fig. 7(d)) is a metastable configuration. The negative pulse first leads to an almost uniform magnetization, caused by injection of a new vortex with opposite curl (Fig. 7(e)). The new vortex reverses the free layer (Fig. 7(f)). The new C state with M_x anti-parallel to the polarizer is not stable at zero current but relaxes relatively slowly into the original uniform configuration.

Recent numerical simulations as well as dynamical experiments using giant magneto-resistance (GMR) measurements have suggested that the Oersted field caused by the charge current produces a transient curled magnetization distribution. Our experiment demonstrates that C states of various shapes are indeed generated. The C state, shown in Fig. 7(d), which is bistable with the uniform state, can solely be reached by injection of a current, but not by application of an external field.

The observed switching mechanism through vortex motion can be viewed as a two step process. First, a C-state is formed by the strong Oersted field. The vortex leads to a non-zero angle between the injected spins and the mag-

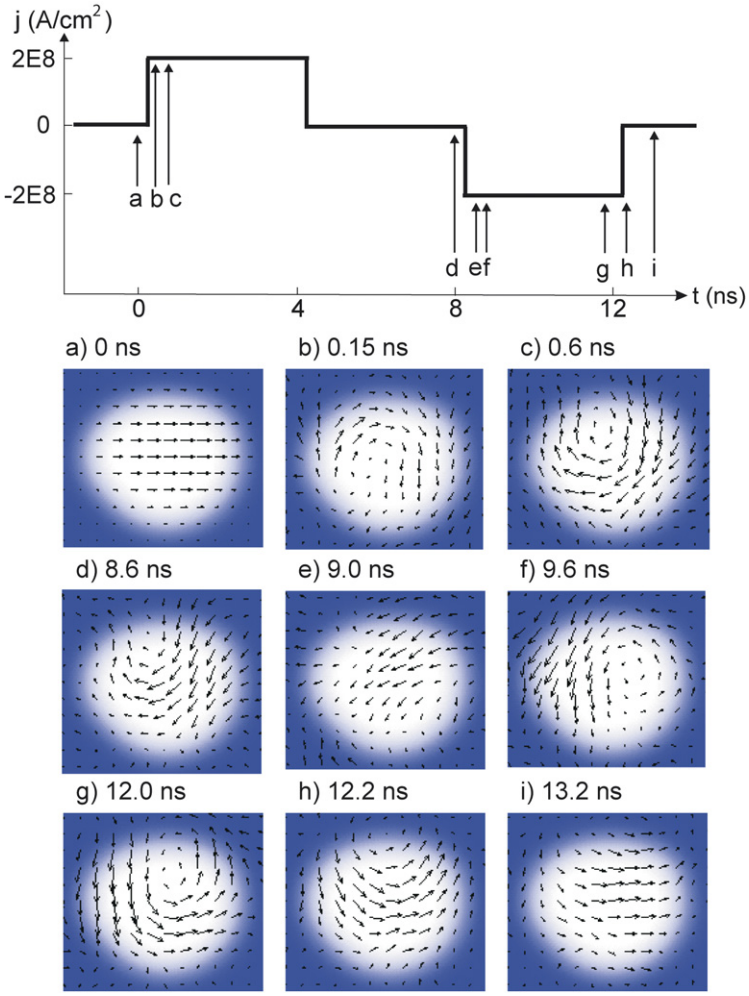

Fig. 7. Evolution of the magnetization during the pulse sequence. The arrows represent the measured magnetization direction. The blue (mid grey) mask indicates the shape of the pillar, reconstructed from absorption images. The uniform anti-parallel configuration (a) is switched into a C state with a parallel M_x component (c). The switching process involves motion of a magnetic vortex, visible in (b). The C state is metastable after the falling edge of the pulse (d) and is reversed by the set pulse into another C state (f). The switching of one C state into another is caused by lateral vortex motion as well, leaving a uniformly magnetized area in the center (e). The C state with its horizontal x component anti-parallel to the polarizer is unstable and relaxes into the uniform state (g)–(i). This relaxation is deterministic but comparatively slow.

netization of the free layer. The spin torque is zero as long as the direction of the injected spins is exactly parallel or anti-parallel to the magnetization of the free layer. The non-zero angle therefore starts the formation and motion of the vortex core across the free layer by spin transfer. Spin transfer amplifies the precessional motion of the magnetization, leading to the formation and a net motion of the vortex across the free layer. Experimentally, the motion of the vortex does not show any gyroscopic motion. The most likely reason for this is that vortex cores with random core magnetization are generated for each cycle of the experiment. The observed trajectory is the average of all trajectories and thus does not reflect the true motion of a single vortex.

New experiments on samples with a free layer of 2 nm thickness show other switching regimes [47]. We observed the response of 200 nm × 100 nm pillars. These samples show full switching by current pulses: the C-state can not be observed in pulsed transport experiments. Still, X-ray images clearly show switching by vortex motion. However, as the size of the pillar is reduced to 150 nm × 100 nm or smaller, the switching mechanism seems not to involve a vortex as the y component of the magnetization does not show any signal during the whole switching time. Future X-ray microscopy experiments will show the details of the different switching mechanisms and their time scales.

4. Summary

As fundamental velocities connect the length scales of nanostructures to the ultrafast time scales, microscopy techniques with high spatial and temporal resolution gain importance. Today's recording technology uses magnetic nanostructures which are switched on sub-nanosecond time scales. X-ray microscopy with synchrotron radiation uniquely offers insight into magneto-dynamics on a length scale only accessible for micromagnetic simulations so far. We have shown that the magnetic vortex plays an important role in magnetism. The vortex can act as a 'hidden parameter' defining the gyroscopic motion of the domain wall crossing in Landau patterns. Van Waeyenberge et al. [27] recently demonstrated resonant, deterministic vortex core switching by a weak RF magnetic field. Surprisingly, the vortex also plays an important role in magnetization switching by spin injection, providing a novel switching mechanism. This mechanism is based on the interplay of the Oersted magnetic field of the spin polarized current and the torque exerted by spin transfer. These experiments show that X-ray microscopy provides a unique tool to see the ultra-fast and the ultra-small.

Acknowledgements

I would like to thank J.P. Strachan, V. Chembrolu, X. Yu, A.A. Tulapurkar, T. Tylisczcak, J. Katine, H.C. Siegmann and J. Stöhr as well as A. Scholl, S.B. Choe and H. Stoll for discussions and collaborations. This work was supported by DOE-BES and by NSF under Grant No. DMR-0203835.

References

[1] J. Stöhr, Y. Wu, B.D. Hermsmeier, M.G. Samant, G.R. Harp, S. Koranda, D. Dunham, B.P. Tonner, Science 259 (5095) (1993) 658–661.
[2] A.L.D. Kilcoyne, T. Tyliszczak, W.F. Steele, S. Fakra, P. Hitchcock, K. Franck, E. Anderson, B. Harteneck, E.G. Rightor, G.E. Mitchell, A.P. Hitchcock, L. Yang, T. Warwick, H. Ade, J. Synchrotron Radiat. 10 (2003) 125–136.
[3] P. Fischer, D.H. Kim, W. Chao, J.A. Liddle, E.H. Anderson, D.T. Attwood, Mater. Today 9 (2006).
[4] M.R. Scheinfein, J. Unguris, M.H. Kelley, D.T. Pierce, R.J. Celotta, Rev. Sci. Instrum. 61 (10) (1990) 2501–2526.
[5] K. Koike, H. Matsuyama, K. Hayakava, Scanning Microsc. (1987) 241–253.
[6] A. Kubetzka, M. Bode, O. Pietzsch, R. Wiesendanger, Phys. Rev. Lett. 88 (5) (2002) 057201-4.
[7] D. Wortmann, S. Heinze, P. Kurz, G. Bihlmayer, S. Blugel, Phys. Rev. Lett. 86 (18) (2001) 4132–4135.
[8] A. Winkler, T. Muhl, S. Menzel, R. Kozhuharova-Koseva, S. Hampel, A. Leonhardt, B. Buchner, J. Appl. Phys. 99 (10) (2006) 104905-1.
[9] W.K. Hiebert, A. Stankiewicz, M.R. Freeman, Phys. Rev. Lett. 79 (6) (1997) 1134–1137.
[10] Y. Acremann, C.H. Back, M. Buess, O. Portmann, A. Vaterlaus, D. Pescia, H. Melchior, Science 290 (5491) (2000) 492–495.
[11] Y. Acremann, M. Buess, C.H. Back, M. Dumm, G. Bayreuther, D. Pescia, Nature 414 (6859) (2001) 51–54.
[12] M. Buess, R. Hollinger, T. Haug, K. Perzlmaier, U. Krey, D. Pescia, M.R. Scheinfein, D. Weiss, C.H. Back, Phys. Rev. Lett. 93 (7) (2004) 077207-4.
[13] M. Buess, T. Haug, M.R. Scheinfein, C.H. Back, Phys. Rev. Lett. 94 (12) (2005) 1–4.
[14] A. Neudert, J. McCord, D. Chumakov, R. Schäber, L. Schultz, Phys. Rev. B 71 (2005).
[15] B.C. Choi, M. Belov, W.K. Hiebert, G.E. Ballentine, M.R. Freeman, Phys. Rev. Lett. 86 (4) (2001) 728–731.
[16] S. Zelakiewicz, A. Krichevsky, M. Johnson, M.R. Freeman, J. Appl. Phys. 91 (10) (2002) 7331–7333.
[17] B.C. Choi, J. Ho, G. Arnup, M.R. Freeman, Phys. Rev. Lett. 95 (23) (2005) 237211-4.
[18] T. Gerrits, H.A.M. van den Berg, J. Hohlfeld, L. Bar, T. Rasing, Nature 418 (6897) (2002) 509–512.
[19] G. Meyer, T. Crecelius, A. Bauer, D. Wegner, I. Mauch, G. Kaindl, J. Microsc. 210 (2003) 209–213.
[20] T. Shinjo, T. Okuno, R. Hassdorf, K. Shigeto, T. Ohno, Science 289 (2000).
[21] A. Wachowiak, J. Wiebe, M. Bode, O. Pietzsch, M. Morgenstern, R. Wiesendanger, Science 298 (2002) 577.
[22] S.B. Choe, Y. Acremann, A. Scholl, A. Bauer, A. Doran, J. Stöhr, H.A. Padmore, Science 304 (2004) 420.
[23] A.A. Thiele, Phys. Rev. Lett. 30 (6) (1973) 230–233.
[24] J. Raabe, C. Quitmann, C.H. Back, F. Nolting, S. Johnson, C. Buehler, Phys. Rev. Lett. 94 (21) (2005) 217204-4.
[25] K.Yu. Guslienko, X.F. Han, D.J. Keavney, R. Divan, S.D. Bader, Magnetic vortex core dynamics in cylindrical ferromagnetic dots, Phys. Rev. Lett. 96 (2006) 067205.
[26] A. Thiaville, J.M. Garcia, R. Dittrich, J. Miltat, T. Schrefl, Phys. Rev. B 67 (9) (2003) 94410-1.
[27] B. Van Waeyenberge, A. Puzic, H. Stoll, K.W. Chou, T. Tyliszczak, R. Hertel, M. Fahnle, H. Bruckl, K. Rott, G. Reiss, I. Neudecker, D. Weiss, C.H. Back, G. Schutz, Nature 444 (7118) (2006) 461–464.
[28] J.C. Slonczewski, J. Magn. Magn. Mater. 159 (1996) L1.
[29] L. Berger, Phys. Rev. B 54 (1996) 9353.
[30] J.E. Wegrowe, D. Kelly, Y. Jaccard, P. Guittienne, J.P. Ansermet, Europhys. Lett. 45 (5) (1999) 626–632.
[31] M. Tsoi, A.G.M. Jansen, J. Bass, W.C. Chiang, M. Seck, V. Tsoi, P. Wyder, Phys. Rev. Lett. 80 (1998) 4281.
[32] E.B. Myers, D. Ralph, J.A. Katine, R.N. Louie, R.A. Buhrman, Science 285 (1999) 867.

[33] J.Z. Sun, J. Magn. Magn. Mater. 202 (1999) 157.
[34] J.A. Katine, F.J. Albert, R.A. Buhrman, E.B. Myers, D.C. Ralph, Phys. Rev. Lett. 84 (2000) 3149.
[35] M. Tsoi, A.G.M. Jansen, J. Bass, W.C. Chiang, V. Tsoi, P. Wyder, Nature 406 (2005) 46.
[36] J. Grollier, V. Cros, A. Hamzic, J.M. George, H. Jaffres, A. Fert, G. Faini, J. Ben Youssef, H. Legall, Appl. Phys. Lett. 78 (2001) 3663.
[37] R.H. Koch, J.A. Katine, J.Z. Sun, Phys. Rev. Lett. 92 (2004) 88302.
[38] I.N. Krivorotov, N.C. Emley, A.G.F. Garcia, J.C. Sankey, S.I. Kiselev, D.C. Ralph, R.A. Buhrman, Phys. Rev. Lett. 93 (2004) 166603.
[39] I.N. Krivorotov, N.C. Emley, J.C. Sankey, S.I. Kiselev, D.C. Ralph, R.A. Buhrman, Science 307 (2005) 228.
[40] T. Devolder, A. Tulapurkar, K. Yagami, P. Crozat, C. Chappert, A. Fukushima, Y. Suzuki, J. Magn. Magn. Mater. 286 (2005) 77.
[41] K.-J. Lee, A. Deac, O. Redon, J.P. Nozieres, B. Dieny, Nature Mater. 3 (12) (2004) 877–881.
[42] S.L. Kiselev, J.C. Sankey, I.N. Krivorotov, N.C. Emley, R.J. Schoelkopf, R.A. Buhrman, Nature 425 (2003) 380.
[43] S.I. Kiselev, J.C. Sankey, I.N. Krivorotov, N.C. Emley, M. Rinkoski, C. Perez, R.A. Buhrman, D.C. Ralph, Phys. Rev. Lett. 93 (2004) 036601.
[44] W.H. Rippard, M.R. Pufall, S. Kaka, S.E. Russek, T.J. Silva, Phys. Rev. Lett. 92 (2004) 027201.
[45] W. Weber, S. Riesen, H.C. Siegmann, Science 291 (5506) (2001) 1015–1018.
[46] Y. Acremann, V. Chembrolu, J.P. Strachan, T. Tyliszczak, J. Stöhr, Rev. Sci. Instrum. 78 (1) (2007) 014702.
[47] J.P. Strachan, et al., 2007, in preparation.